Networks and Heterogeneous Media

https://www.aimspress.com/journal/nhm

NHM, 21(3): 755–772.
DOI: 10.3934/nhm.2026032
Received: 13 January 2026
Revised: 02 April 2026
Accepted: 07 April 2026
Published: 27 April 2026

Research article

Stability of implicit defect correction methods based on the new class of BDF methods

Lin Yao[1], **Xindong Zhang**[2,*] **and Xianzhu Li**[1,]

[1] School of Mathematical Sciences, Xinjiang Normal University, Urumqi 830017, China

[2] College of Big Data Statistics, Guizhou University of Finance and Economics, Guiyang 550025, China

* **Correspondence:** E-mail: liaoyuan1126@163.com.

Abstract: This paper presents a class of novel, high-order, A-stable defect correction schemes. These schemes are grounded in a newly developed, more versatile class of BDF approaches, which utilize Taylor expansions at time $t_{n+\beta}$ with $\beta > 1$ being an adjustable parameter. The ranges for the stability parameters of these newly proposed defect correction schemes are specified to ensure A-stability. Additionally, numerical experiments are given to illustrate the precision and robustness of the schemes when addressing stiff problems.

Keywords: A-stable; defect correction schemes; BDF approaches; Taylor expansions; stiff problems

1. Introduction

In this paper, we consider the deferred correction (DC) methods based on a new class of the backward differentiation formula (BDF) approaches for stiff problems [1] in the form

$$\begin{cases} \phi_t = F(t, \phi), & 0 < t < T, \\ \phi(0) = \phi_0, \end{cases} \tag{1.1}$$

where $F(t, \phi)$ is a function of the variables t and ϕ, and T denotes the final time. A stiff problem refers to differential systems of equations that exhibit high instability and significant differences in time scales. These problems are widely applied in physical fields such as materials science, fluid mechanics, and mechanical systems in [2, 3]. A-stability is a crucial property when solving stiff problems in [4]. The conventional implicit methods have A-stability features, such as such as the backward Euler method and implicit Runge-Kutta (RK) methods in [5, 6]. These methods can maintain stability with relatively large time steps and effectively handle the rapidly decaying components in stiff problems.

However, although implicit RK schemes have excellent stability and can theoretically be constructed to arbitrary order, the derivation and selection of their Butcher coefficients remain challenging, which significantly raises the threshold for constructing high-order schemes. Linear multistep methods, such as the widely used backward differentiation formulas (BDF) approaches, are also very effective for simulating stiff problems; nevertheless, high-order schemes have poor stability in [7–9]. In addition, Dahlquist's well-known theorem [10] reveals that linear multistep methods with an order higher than 2 cannot be A-stable. Therefore, the attractiveness of the high-order multistep methods decreases. In [11], Yao and his colleagues introduced three types of implicit DC methods based on the classical BDF methods, aiming to devise high-order, A-stable multistep schemes, and provided some stability conditions.

The DC or spectral deferred correction (SDC) methods are also among the main methods for the above stiff problems. The classical implicit DC or SDC methods were originally proposed and refined in [12, 13]. In [14], Minion originally developed a linear implicit SDC method to approximate the stiff system. In [15], Layton delved into the study of semi-implicit Picard DC methods, emphasizing their effectiveness. In [16], Guo and her colleagues developed a novel class of semi-implicit SDC schemes tailored for nonlinear stiff problems. In [17], Yao and his colleagues introduce two types of L-stable implicit SDC methods for solving stiff problems, which are based on the second-order Crank-Nicolson method. Due to stability reasons, DC methods, which are based on first- or second-order methods, are used to achieve fourth-order or higher [18]. Compared to general implicit RK methods, implicit DC methods require solving linear or nonlinear systems of equations with much smaller dimensions at each step.

Traditionally, when computing solutions at time t_{n+1}, classical BDF methods generally rely on Taylor expansion formulae at time $t_{n+\beta}, \beta \in \{0, 1\}$. Huang and Shen [19] developed a novel class of BDF methods, which also employ Taylor expansion formulas at $t_{n+\beta}, \beta \geq 1$, with the aim of improving the stability of the classical BDF methods. At $\beta = 1$, the new BDF methods are equal to the classical BDF methods. Inspired by the key idea, we develop several innovative classes of multistep, high-order, implicit schemes. Specifically, we propose three schemes: the novel BDF-DC$_3^3$/DC$_5^4$ approach, the BDF-DC$_2^3$/DC$_3^4$ method, and the BDF-DC$_2^4$ technique. Leveraging Schur theory [20], we determine the appropriate ranges for the stability parameters in these schemes, aiming to achieve larger stability regions than the classical BDF-DC schemes. Furthermore, we provide an example for the stiff system to validate the effectiveness and robustness of the novel schemes.

The remaining sections of this article are structured as follows. We provide an overview of the proposed A-stable implicit schemes in Section 2. The A-stability analysis of the introduced new approaches is described in Section 3. Section 4 presents some numerical experiments. Some conclusions are outlined in Section 5.

2. The novel high-order DC methods

This section begins by constructing a new class of BDF schemes specifically designed for Eq (1.1). Given an integer $k \geq 2$, and with $t_n = n\Delta t$ (where Δt is time step), we can derive the following general

formula by applying the Taylor expansion at $t_{n+\beta}$ where $\beta \geq 1$:

$$\phi(t_{n+1-i}) = \sum_{m=0}^{k-1}[(1-i-\beta)\Delta t]^m \frac{\phi^m(t_{n+\beta})}{m!} + O(\Delta t^k) \quad \text{for} \quad k \geq i \geq 0. \tag{2.1}$$

Based on Eq (2.1), we can deduce the following implicit difference formulae to approximate $\partial_t\phi(t_{n+\beta})$ and $\phi(t_{n+\beta})$:

$$\begin{aligned} &\frac{1}{\Delta t}\sum_{q=0}^{k} a_{k,q}(\beta)\phi(t_{n+1-k+q}) = \partial_t\phi(t_{n+\beta}) + O(\Delta t^k), \\ &\sum_{q=0}^{k-1} b_{k,q}(\beta)\phi(t_{n+2-k+q}) = \phi(t_{n+\beta}) + O(\Delta t^k), \end{aligned} \tag{2.2}$$

where the coefficients $a_{k,q}(\beta)$ and $b_{k,q}(\beta)$ can be uniquely identified by solving a linear system that incorporates a Vandermonde matrix. Then, a new class of BDF scheme for Eq (1.1) is given by

$$\frac{1}{\Delta t}\sum_{q=0}^{k} a_{k,q}(\beta)\phi_{n+1-k+q} = F(t_{n+\beta}, \sum_{q=0}^{k-1} b_{k,q}(\beta)\phi_{n+2-k+q}), \quad k \geq 2. \tag{2.3}$$

Here, we will derive three novel implicit BDF-DC schemes. For the prediction stages: We employ the above new BDF scheme (2.3) with $k = 2$ and $k = 3$, respectively. We then obtain the initial approximate solutions $\phi^{(2)}(t)$ and $\phi^{(3)}(t)$, respectively. For a more detailed derivation process, please refer to [19]. For the deferred correction stages, given initial values $\phi_{n-2}, \phi_{n-1}, \phi_n$, we first integrate Eq (1.1) from 0 to t given by

$$\phi(t) = \phi_0 + \int_0^t F(\tau, \phi(\tau))d\tau. \tag{2.4}$$

Given the initial approximation $\phi^{(2)}(t)$, we define the error equation as $\delta(t) = \phi(t) - \phi^{(2)}(t)$. We then define the residual equation as follows:

$$\varepsilon(t, \phi^{(2)}) = \phi_0 + \int_0^t F(\tau, \phi^{(2)}(\tau))d\tau - \phi^{(2)}(t). \tag{2.5}$$

Substituting $\phi(t) = \phi^{(2)}(t) + \delta(t)$ into Eq (2.4), we have

$$\delta(t) = \phi_0 + \int_0^t F(\tau, \phi^{(2)}(\tau) + \delta(\tau))d\tau - \phi^{(2)}(t). \tag{2.6}$$

By combining the residual equation (2.5) with the error equation (2.6), we have

$$\delta(t) = \int_0^t F(\tau, \phi^{(2)}(\tau) + \delta(\tau)) - F(\tau, \phi^{(2)}(\tau))d\tau + \varepsilon(t, \phi^{(2)}). \tag{2.7}$$

For the given interval $[t_{n-1}, t_{n+1}]$, we substitute $t = t_{n-1}$ and $t = t_{n+1}$ into Eq (2.7) as follows:

$$\begin{aligned}\delta(t_{n-1}) &= \int_0^{t_{n-1}} F(\tau, \phi^{(2)}(\tau) + \delta(\tau)) - F(\tau, \phi^{(2)}(\tau))d\tau + \varepsilon(t_{n-1}, \phi^{(2)}),\\ \delta(t_{n+1}) &= \int_0^{t_{n+1}} F(\tau, \phi^{(2)}(\tau) + \delta(\tau)) - F(\tau, \phi^{(2)}(\tau))d\tau + \varepsilon(t_{n+1}, \phi^{(2)}).\end{aligned} \tag{2.8}$$

Let the second equation in Eq (2.8) substrate into the first equation in Eq (2.8) as follows:

$$\begin{aligned}\delta(t_{n+1}) = \delta(t_{n-1}) &+ \int_{t_{n-1}}^{t_{n+1}} F(\tau, \phi^{(2)}(\tau) + \delta(\tau)) - F(\tau, \phi^{(2)}(\tau))d\tau\\ &+ \varepsilon(t_{n+1}, \phi^{(2)}) - \varepsilon(t_{n-1}, \phi^{(2)}),\end{aligned} \tag{2.9}$$

where we use $\delta_{n+1}^{(2)}$ to approximate $\delta(t_{n+1})$, $\phi_{n+1}^{(2)}$ to approximate $\phi(t_{n+1})$, and define $\phi_{n+1}^{(3)} = \phi_{n+1}^{(2)} + \delta_{n+1}^{(2)}$. For the correction term in Eq (2.9), we numerically approximate the exact integral using the following stabilization term with the tunable parameter η:

$$\int_{t_{n-1}}^{t_{n+1}} F(\tau, \phi^{(2)}(\tau) + \delta(\tau)) - F(\tau, \phi^{(2)}(\tau))d\tau \approx \eta\Delta t(F(t_{n+1}, \phi_{n+1}^{(3)}) - F(t_{n+1}, \phi_{n+1}^{(2)})). \tag{2.10}$$

For the approximation of the residual term in Eq (2.9), we first define the numerical integral as:

$$I_0^3(F; \phi_{n-1}, \phi_n, \phi_{n+1}^{(2)}) \approx \int_{t_{n-1}}^{t_{n+1}} F(\tau, \phi^{(2)}(\tau))d\tau, \tag{2.11}$$

and then obtain the following residual approximation:

$$\varepsilon_{n+1} - \varepsilon_n = I_0^3(F; \phi_{n-1}, \phi_n, \phi_{n+1}^{(2)}) - \phi_{n+1}^{(2)} + \phi_n^{(2)}. \tag{2.12}$$

We then substitute Eqs (2.10) and (2.12) into Eq (2.9), obtaining the following third-order scheme:

$$\phi_{n+1}^{(3)} = \phi_{n-1} + \eta\Delta t(F(t_{n+1}, \phi_{n+1}^{(3)}) - F(t_{n+1}, \phi_{n+1}^{(2)})) + I_0^3(F; \phi_{n-1}, \phi_n, \phi_{n+1}^{(2)}), \tag{2.13}$$

When we update Eq (2.13) again, we obtain the fourth-order scheme:

$$\phi_{n+1}^{(4)} = \phi_{n-1} + \eta\Delta t(F(t_{n+1}, \phi_{n+1}^{(4)}) - F(t_{n+1}, \phi_{n+1}^{(3)})) + I_0^3(F; \phi_{n-1}, \phi_n, \phi_{n+1}^{(3)}). \tag{2.14}$$

Therefore, we rigorously derive the novel third/fourth-order BDF-DC$_2^3$/DC$_3^4$ scheme. To facilitate readers' understanding, we rewrite the third/fourth-order scheme in the form of Eq (2.16). We then apply the process similar to that in Eqs (2.4)–(2.12) to derive the novel BDF-DC$_3^3$/DC$_5^4$ and BDF-DC$_2^4$ schemes, which are given in Eqs (2.15) and (2.17), respectively.

- **The novel BDF-DC$_3^3$/DC$_5^4$ scheme:**

$$\begin{aligned}\phi_{n+\frac{1}{2}}^{(2)} &= -\frac{4\beta_1 - 1}{8\beta_1 + 4}\phi_{n-1} + \frac{12\beta_1 + 3}{8\beta_1 + 4}\phi_n + \frac{3\Delta t}{8\beta_1 + 4}F(t_{n+\beta_1}, 2\beta_1\phi_{n+\frac{1}{2}}^{(2)} + (1 - 2\beta_1)\phi_n),\\ \phi_{n+1}^{(2)} &= -\frac{2\beta_2 - 1}{2\beta_2 + 1}\phi_{n-1} + \frac{4\beta_2}{2\beta_2 + 1}\phi_n + \frac{2\Delta t}{2\beta_2 + 1}F(t_{n+\beta_2}, \beta_2\phi_{n+1}^{(2)} - (\beta_2 - 1)\phi_n),\\ \phi_{n+1}^{(3)} &= \phi_n + \alpha_1\Delta t(F(t_{n+1}, \phi_{n+1}^{(3)}) - F(t_{n+1}, \phi_{n+1}^{(2)})) + I_0^2(F; \phi_n, \phi_{n+\frac{1}{2}}^{(2)}, \phi_{n+1}^{(2)}),\\ \phi_{n+\frac{1}{2}}^{(3)} &= \phi_n + \alpha_2\Delta t(F(t_{n+\frac{1}{2}}, \phi_{n+\frac{1}{2}}^{(3)}) - F(t_{n+\frac{1}{2}}, \phi_{n+\frac{1}{2}}^{(2)})) + I_0^1(F; \phi_n, \phi_{n+\frac{1}{2}}^{(2)}, \phi_{n+1}^{(2)}),\\ \phi_{n+1}^{(4)} &= \phi_n + \alpha_1\Delta t(F(t_{n+1}, \phi_{n+1}^{(4)}) - F(t_{n+1}, \phi_{n+1}^{(3)})) + I_0^2(F; \phi_n, \phi_{n+\frac{1}{2}}^{(3)}, \phi_{n+1}^{(3)}).\end{aligned} \tag{2.15}$$

• **The novel BDF-DC$_2^3$/DC$_3^4$ scheme:**

$$\begin{aligned}
\phi_{n+1}^{(2)} &= -\frac{2\beta_2-1}{2\beta_2+1}\phi_{n-1} + \frac{4\beta_2}{2\beta_2+1}\phi_n + \frac{2\Delta t}{2\beta_2+1}F(t_{n+\beta_2}, \beta_2\phi_{n+1}^{(2)} - (\beta_2-1)\phi_n),\\
\phi_{n+1}^{(3)} &= \phi_{n-1} + \eta\Delta t(F(t_{n+1}, \phi_{n+1}^{(3)}) - F(t_{n+1}, \phi_{n+1}^{(2)})) + I_0^3(F; \phi_{n-1}, \phi_n, \phi_{n+1}^{(2)}),\\
\phi_{n+1}^{(4)} &= \phi_{n-1} + \eta\Delta t(F(t_{n+1}, \phi_{n+1}^{(4)}) - F(t_{n+1}, \phi_{n+1}^{(3)})) + I_0^3(F; \phi_{n-1}, \phi_n, \phi_{n+1}^{(3)}).
\end{aligned} \tag{2.16}$$

• **The novel BDF-DC$_2^4$ scheme:**

$$\begin{aligned}
\phi_{n+1}^{(3)} &= \frac{3\beta_2^2-1}{3\beta_2^2+6\beta_2+2}\phi_{n-2} - \frac{9\beta_2^2+6\beta_2-6}{3\beta_2^2+6\beta_2+2}\phi_{n-1} + \frac{9\beta_2^2+12\beta_2-3}{3\beta_2^2+6\beta_2+2}\phi_n\\
&\quad + \frac{6\Delta t}{3\beta_2^2+6\beta_2+2}F(t_{n+\beta_2}, \frac{\beta_2^2+\beta_2}{2}\phi_{n+1}^{(3)} - (\beta_2^2-1)\phi_n + \frac{\beta_2^2-\beta_2}{2}\phi_{n-1}),\\
\phi_{n+1}^{(4)} &= \phi_{n-1} + \gamma\Delta t(F(t_{n+1}, \phi_{n+1}^{(4)}) - F(t_{n+1}, \phi_{n+1}^{(3)})) + I_0^3(F; \phi_{n-1}, \phi_n, \phi_{n+1}^{(3)}),
\end{aligned} \tag{2.17}$$

where α_1, α_2, η, γ, $\beta_1 \geq \frac{1}{2}$, and $\beta_2 \geq 1$ are the stability parameters, and $\phi_{n+p}^{(l)}$ denotes the lth-order approximation of the solution $\phi(t_{n+p})$, where $l = 2, 3$ or 4. I_0^1, I_0^2, and I_0^3 are defined as the integral approximations on $[t_n, t_{n+\frac{1}{2}}]$, $[t_n, t_{n+1}]$, and $[t_{n-1}, t_{n+1}]$, respectively, as introduced in [11]. In the next section, we analyze the stability for the proposed novel schemes, estimating the ranges of the parameters α_1, α_2, η, and γ, which control the stability of the novel schemes.

3. Stability of the novel high-order DC methods

We analyze the stability of the new methods with Schur theory [20]. For establishing stability criteria of the schemes (2.15)–(2.17), we can use the similar analytical tool that is specified in the literature [11]. Next, we utilize the theoretical tool to establish the conditions.

Let $\lambda = r\cos\theta + \mathrm{i}r\sin\theta$, where $r > 0$ and $\theta \in (\frac{\pi}{2}, \frac{3\pi}{2})$. For the BDF-DC$_3^3$ scheme in Eq (2.15) ($\phi_{n+1} = \phi_{n+1}^{(3)}$), we can obtain its characteristic polynomial as follows:

$$f(z) = a_2z^2 + a_1z + a_0, \tag{3.1}$$

where the derivation process of the detailed expressions of the coefficients a_2, a_1, and a_3 is carried out using **Proposition 3.1** in [11], given by

$$\begin{aligned}
a_2 &= 6(-2-4\beta_1-4\beta_2-8\beta_1\beta_2) + 6(2\alpha_1+3\beta_1+4\alpha_1\beta_1+4\beta_2+4\alpha_1\beta_2+14\beta_1\beta_2\\
&\quad + 8\alpha_1\beta_1\beta_2)\lambda + 6(-3\alpha_1\beta_1-4\alpha_1\beta_2-6\beta_1\beta_2-14\alpha_1\beta_1\beta_2)\lambda^2 + 36\alpha_1\beta_1\beta_2\lambda^3,\\
a_1 &= 12+24\beta_1+24\beta_2+48\beta_1\beta_2 + (8+10\beta_1-48\alpha_1\beta_2-12\beta_1\beta_2-96\alpha_1\beta_1\beta_2)\lambda\\
&\quad + (10-24\alpha_1-7\beta_1-48\alpha_1\beta_1-8\beta_2+24\alpha_1\beta_2-70\beta_1\beta_2+120\alpha_1\beta_1\beta_2)\lambda^2 +\\
&\quad (-6\beta_1+36\alpha_1\beta_1-12\beta_2+36\beta_1\beta_2-36\alpha_1\beta_1\beta_2)\lambda^3,\\
a_0 &= (4-12\alpha_1-4\beta_1-24\alpha_1\beta_1+24\alpha_1\beta_2-24\beta_1\beta_2+48\alpha_1\beta_1\beta_2)\lambda + (-3\beta_1\\
&\quad + 18\alpha_1\beta_1-4\beta_2+22\beta_1\beta_2-36\alpha_1\beta_1\beta_2)\lambda^2.
\end{aligned}$$

We say that the above third-order scheme is A-stable if it requires

$$b_0 + b_1\cos\theta + b_2\cos^2\theta + b_3\cos^3\theta + b_4\cos^4\theta + b_5\cos^5\theta + b_6\cos^6\theta > 0. \tag{3.2}$$

Here, $b_0, b_1, \cdots, b_6$ depend on $\alpha_1, \beta_1, \beta_2$ and r. We rely on sufficient conditions: $b_0, b_2, b_4, b_6 \geq 0$ and $b_1, b_3, b_5 \leq 0$ for arbitrary $r > 0$ in the left plane, and solve the above inequality (3.2). As a result, we obtain the ranges: $\beta_1 \geq \frac{1}{2}, \beta_2 \geq 1$ and $\alpha_1 \geq (\alpha_1)_{\min}$, where

$$(\alpha_1)_{\min} = \max\left(\frac{-\beta_1 - 2\beta_2 + 6\beta_1\beta_2}{-6\beta_1 + 12\beta_1\beta_2}, \frac{-7 + 7\beta_1 + 6\beta_2 + 54\beta_1\beta_2}{-24 - 48\beta_1 + 72\beta_2 + 144\beta_1\beta_2}\right).$$

Similarly, for the novel BDF-DC$_5^4$ scheme in Eq (2.15), it is A-stable if $\alpha_1 \geq (\alpha_1)_{\min}$ and $\alpha_2 \geq (\alpha_2)_{\min}$, where

$$(\alpha_2)_{\min} = \frac{\alpha_1\beta_1 - 4\alpha_1\beta_2 + 12\alpha_1\beta_1\beta_2}{\beta_1 - 12\alpha_1\beta_1 + 36\alpha_1^2\beta_1 + 2\beta_2 - 24\alpha_1\beta_2 - 6\beta_1\beta_2 + 72\alpha_1\beta_1\beta_2}.$$

The scheme is also L-stable if the roots z_1 and z_2 additionally satisfy the following conditions:

$$\begin{aligned}
&\lim_{Re(\lambda)\to-\infty} |z_1| = 0,\\
&\lim_{Re(\lambda)\to-\infty} |z_2| = \Big|\frac{1}{72\alpha_1^2\alpha_2\beta_1\beta_2}(\alpha_1\beta_1 - \alpha_2\beta_1 + 12\alpha_1\alpha_2\beta_1 - 36\alpha_1^2\alpha_2\beta_1 - 4\alpha_1\beta_2 - 2\alpha_2\beta_2\\
&\qquad + 24\alpha_1\alpha_2\beta_2 + 12\alpha_1\beta_1\beta_2 + 6\alpha_2\beta_1\beta_2 - 72\alpha_1\alpha_2\beta_1\beta_2 + 36\alpha_1^2\alpha_2\beta_1\beta_2)\Big| = 0.
\end{aligned} \tag{3.3}$$

The first condition is satisfied automatically, while the second condition introduces a new constraint on the stability parameters α_1, α_2 and β_1, β_2. Consequently, we derive the following equality relationship:

$$\begin{aligned}
&\alpha_2 = (z_2)_{\text{lim}},\\
&(z_2)_{\text{lim}} = \Big|\frac{\alpha_1\beta_1 - 4\alpha_1\beta_2 + 12\alpha_1\beta_1\beta_2}{\beta_1 - 12\alpha_1\beta_1 + 36\alpha_1^2\beta_1 + 2\beta_2 - 24\alpha_1\beta_2 - 6\beta_1\beta_2 + 72\alpha_1\beta_1\beta_2 - 36\alpha_1\beta_1\beta_2 - 36\alpha_1^2\beta_1\beta_2}\Big|.
\end{aligned}$$

For the novel BDF-DC$_2^3$ scheme in Eq (2.16), we can say that it is A-stable as long as it requires $\beta_2 \geq 1$ and $\eta \geq (\eta_1)_{\min}$, where $(\eta_1)_{\min} = \frac{-1+4\beta_2}{-3+6\beta_2}$. And, for the novel BDF-DC$_3^4$ scheme in Eq (2.16), it is stiff-stable as long as it requires $\beta_2 \geq 1$, $\eta \geq (\eta_2)_{\min}$, where $(\eta_2)_{\min} = \frac{-1+4\beta_2+\sqrt{-2\beta_2+8\beta_2^2}}{-3+6\beta_2}$, and it also satisfies $D = D_1, D_1 = \sqrt{-\frac{C}{B}}$ when $A = 0$ or $D = D_1, D_1 = \sqrt{\frac{-B+\sqrt{B^2-4AC}}{2A}}$ when $A \neq 0$, where

$$\begin{aligned}
A &= \beta_2^2(-1 + 10\beta_2 - 24\beta_2^2) + \beta_2^2(12 - 120\beta_2 + 288\beta_2^2)\eta + \beta_2^2(-54 + 468\beta_2 - 972\beta_2^2)\eta^2\\
&\quad + \beta_2^2(108 - 648\beta_2 + 648\beta_2^2)\eta^3 + \beta_2^2(-81 + 162\beta_2)\eta^4 > 0,\\
B &= -1 + 16\beta_2 - 87\beta_2^2 + 246\beta_2^3 - 396\beta_2^4 + (12 - 120\beta_2 + 324\beta_2^2 - 108\beta_2^3 + 216\beta_2^4)\eta\\
&\quad + (-36 + 162\beta_2 - 126\beta_2^2 - 162\beta_2^3 + 972\beta_2^4)\eta^2 + (-108\beta_2 + 108\beta_2^2 + 648\beta_2^3)\eta^3 \geq 0,\\
C &= -9\beta_2(1 + 2\beta_2)(2 - 11\beta_2 + 30\beta_2^2) - 9\beta_2(1 + 2\beta_2)(-12 + 12\beta_2 + 72\beta_2^2)\eta \leq 0.
\end{aligned}$$

For the novel BDF-DC$_2^4$ scheme in Eq (2.17), its characteristic polynomial $f(z)$ is a cubic polynomial. It can be reduced to the quadratic polynomial (3.1) by using **Definition 3.1** in [11]. Likewise, the scheme achieves A(α)-stability exclusively when the coefficients in Eq (3.1) adhere to **Proposition 3.1** in [11], resulting in

$$c_0 + c_1 r + c_2 r^2 + c_3 r^3 + c_4 r^4 + c_5 r^5 + c_6 r^6 + c_7 r^7 + c_8 r^8 + c_9 r^9 + c_{10} r^{10} > 0, \tag{3.4}$$

where the coefficients $c_0, c_1, \cdots, c_{10}$ are complex expressions depending on γ, β_2, and $\cos\theta$. By solving Eq (3.4) based on the sufficient condition: $c_0, c_2, c_4, c_6, c_8, c_{10} \geq 0$ and $c_1, c_3, c_5, c_7, c_9 \geq 0$ for any r in the left plane, we derive the stability conditions: $\beta_2 \geq 1, \gamma \geq (\gamma)_{\min}$, $(\gamma)_{\min} = \frac{-1+\beta_2+3\beta_2^2}{-3+6\beta_2^2}$, and $\alpha = \arccos\sqrt{-\frac{G}{H}}$, where

$$\begin{aligned}
G &= (-1+3\gamma)^2((1+\beta_2)^2(-1+\beta_2+3\beta_2^2)(-1+3\beta_2+3\beta_2^2)(1-3\beta_2+6\beta_2^2+9\beta_2^3)^2 \\
&\quad + (-6(1+\beta_2)^2(2-14\beta_2+28\beta_2^2+12\beta_2^3-81\beta_2^4+135\beta_2^5-135\beta_2^6-594\beta_2^7 \\
&\quad + 135\beta_2^8+648\beta_2^9+243\beta_2^{10}))\gamma + (9(6-16\beta_2-48\beta_2^2+138\beta_2^3+310\beta_2^4 \\
&\quad - 102\beta_2^5-546\beta_2^6-360\beta_2^7+207\beta_2^8+864\beta_2^9+999\beta_2^{10}+486\beta_2^{11}+81\beta_2^{12}))\gamma^2 \\
&\quad + (54(-2+2\beta_2+24\beta_2^2-10\beta_2^3-107\beta_2^4-3\beta_2^5+246\beta_2^6+234\beta_2^7+63\beta_2^8))\gamma^3 \\
&\quad + (81(1+2\beta_2)^2(-1+\beta_2+3\beta_2^2)(-1+3\beta_2+3\beta_2^2))\gamma^4), \\
H &= 3\beta_2(1+\beta_2)(12\beta_2(1+\beta_2)(-1+3\beta_2)(-1+3\beta_2^2)(-1+\beta_2+3\beta_2^2)(-1+3\beta_2+3\beta_2^2) \\
&\quad + (-2(-4+120\beta_2-291\beta_2^2-1254\beta_2^3+2097\beta_2^4+5166\beta_2^5-2970\beta_2^6-6696\beta_2^7+1377\beta_2^8 \\
&\quad + 3564\beta_2^9+729\beta_2^{10}))\gamma + (3(-44+553\beta_2+513\beta_2^2-6870\beta_2^3-6792\beta_2^4+21006\beta_2^5 \\
&\quad + 26262\beta_2^6-3537\beta_2^7-7641\beta_2^8+2592\beta_2^9+1782\beta_2^{10}))\gamma^2 + (-18(-48+250\beta_2+1402\beta_2^2 \\
&\quad - 2034\beta_2^3-10566\beta_2^4-1152\beta_2^5+16965\beta_2^6+11610\beta_2^7+891\beta_2^8+324\beta_2^{10}))\gamma^3 + (27(-104 \\
&\quad + 46\beta_2+2746\beta_2^2+2898\beta_2^3-12096\beta_2^4-17919\beta_2^5+1683\beta_2^6+10179\beta_2^7+3807\beta_2^8+405\beta_2^9 \\
&\quad + 81\beta_2^{10}))\gamma^4 + (162(28+90\beta_2-373\beta_2^2-1422\beta_2^3-123\beta_2^4+2493\beta_2^5+2007\beta_2^6+540\beta_2^7 \\
&\quad + 54\beta_2^8))\gamma^5 + (729(-1+2\beta_2)(4+33\beta_2+91\beta_2^2+90\beta_2^3+24\beta_2^4))\gamma^6).
\end{aligned}$$

Table 1. The stability ranges of α_1, α_2, η, and γ for the novel BDF-DC schemes.

Schemes	A(α)-stability	L-stability	Stiff-stability
BDF-DC$_3^3$	$\alpha_1 \geq (\alpha_1)_{\min}$, $\alpha = \frac{\pi}{2}$	–	–
BDF-DC$_2^3$	$\eta \geq (\eta_1)_{\min}$, $\alpha = \frac{\pi}{2}$	–	–
BDF-DC$_3^4$	–	–	$\eta \geq (\eta_2)_{\min}$, $D = D_1$
BDF-DC$_2^4$	$\gamma \geq (\gamma)_{\min}$, $\alpha = \arccos\sqrt{-\frac{G}{H}}$	–	–
BDF-DC$_5^4$	$\alpha_1 \geq (\alpha_1)_{\min}$, $\alpha_2 \geq (\alpha_2)_{\min}$, $\alpha = \frac{\pi}{2}$	$\alpha_1 \geq (\alpha_1)_{\min}$, $\alpha_2 = (z_2)_{\lim}$, $\alpha = \frac{\pi}{2}$	–

Table 1 presents the ranges of α_1, α_2, η, and γ for newly introduced BDF-DC schemes in different stability regions. Figures 1 and 2 illustrate the stability regions of the BDF-DC$_3^3$ and BDF-DC$_5^4$ schemes, respectively, for specific stability parameter values α_1, α_2 and β_1, β_2 as outlined in Table 1. Notably, all these schemes exhibit A-stability. As shown in Figures 1 and 2, the stability regions fully encompass the entire outer area bounded by contour 1. Figures 3–5 convey the same information in the BDF-DC$_2^3$ (A-stable), BDF-DC$_3^4$ (stiff-stable), and BDF-DC$_2^4$ (A(α)-stable) schemes, utilizing different stability parameter values η, γ and β_1, β_2 as specified in Table 1. From these figures, we can conclude that the proposed novel BDF-DC methods have larger stability regions than the classical BDF-DC schemes.

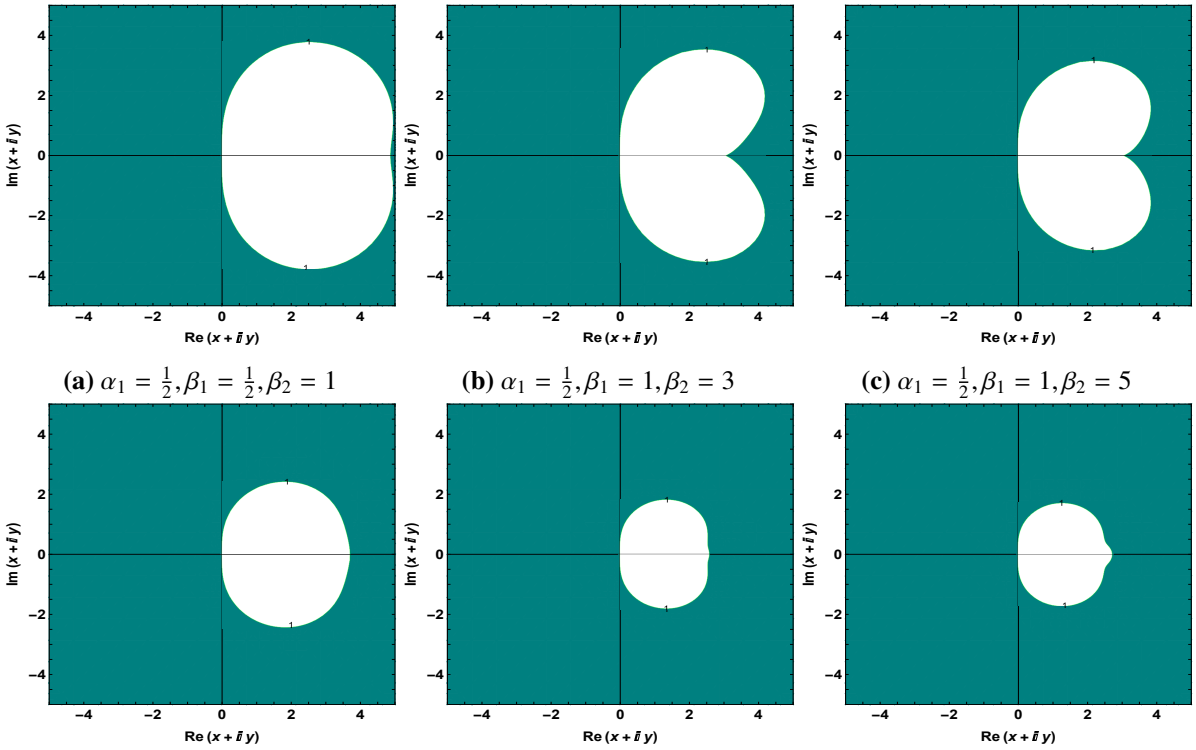

(a) $\alpha_1 = \frac{1}{2}, \beta_1 = \frac{1}{2}, \beta_2 = 1$ **(b)** $\alpha_1 = \frac{1}{2}, \beta_1 = 1, \beta_2 = 3$ **(c)** $\alpha_1 = \frac{1}{2}, \beta_1 = 1, \beta_2 = 5$

(d) $\alpha_1 = 1, \beta_1 = \frac{1}{2}, \beta_2 = 1$ **(e)** $\alpha_1 = 1, \beta_1 = 1, \beta_2 = 3$ **(f)** $\alpha_1 = 1, \beta_1 = 1, \beta_2 = 5$

Figure 1. A-stability regions with different stability parameters α_1, β_1, and β_2. (a) and (d): The classical BDF-DC$_3^3$ scheme; (b), (c), (e), and (f): The novel BDF-DC$_3^3$ scheme.

Remark 1. *It is worth noting that for the newly introduced BDF-DC schemes, we can obtain better stability results and bigger stability regions from Figures 1–5 compared to the classical BDF-DC schemes* ($\beta_1 = \frac{1}{2}, \beta_2 = 1$). *From Figures 1–5, we can observe that Figures (a) and (d) show the stability region contour plots for the classical BDF-DC schemes, while the other plots depict the stability regions for the novel BDF-DC schemes.*

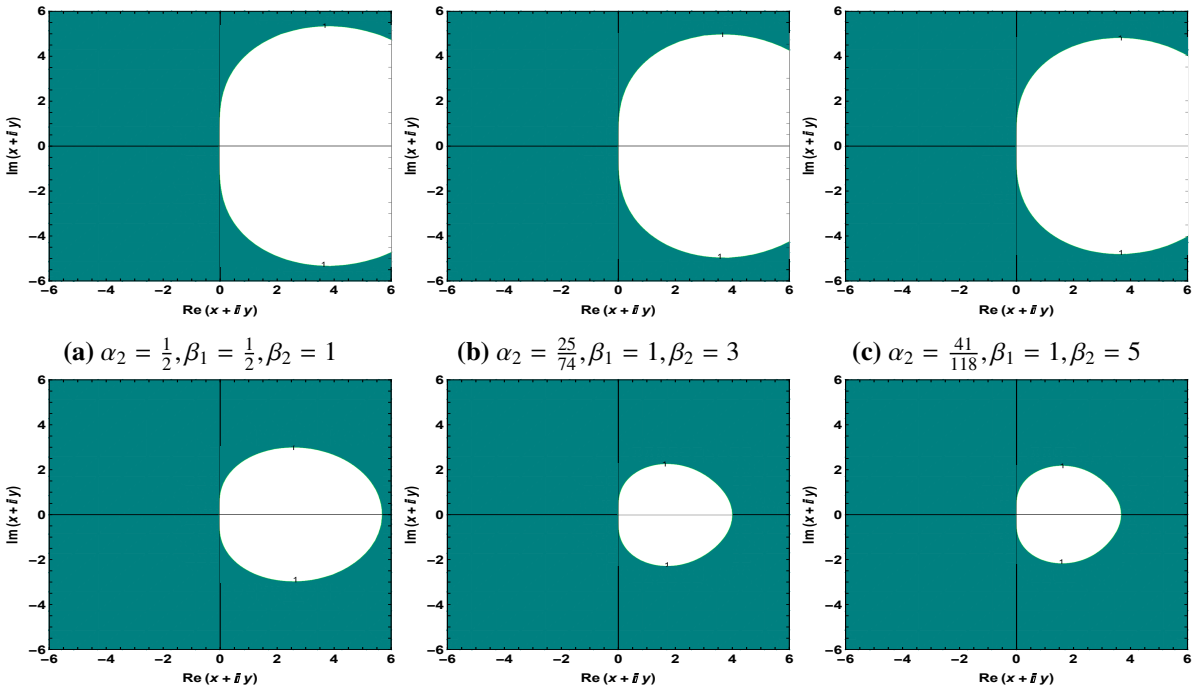

(a) $\alpha_2 = \frac{1}{2}, \beta_1 = \frac{1}{2}, \beta_2 = 1$ **(b)** $\alpha_2 = \frac{25}{74}, \beta_1 = 1, \beta_2 = 3$ **(c)** $\alpha_2 = \frac{41}{118}, \beta_1 = 1, \beta_2 = 5$

(d) $\alpha_2 = \frac{5}{11}, \beta_1 = \frac{1}{2}, \beta_2 = 1$ **(e)** $\alpha_2 = \frac{25}{49}, \beta_1 = 1, \beta_2 = 3$ **(f)** $\alpha_2 = \frac{41}{65}, \beta_1 = 1, \beta_2 = 5$

Figure 2. L-stability regions with different stability parameters $\alpha_1, \alpha_2, \beta_1$, and β_2. (a) and (d): The classical BDF-DC$_5^4$ scheme; (b), (c), (e), and (f): The novel BDF-DC$_5^4$ scheme.

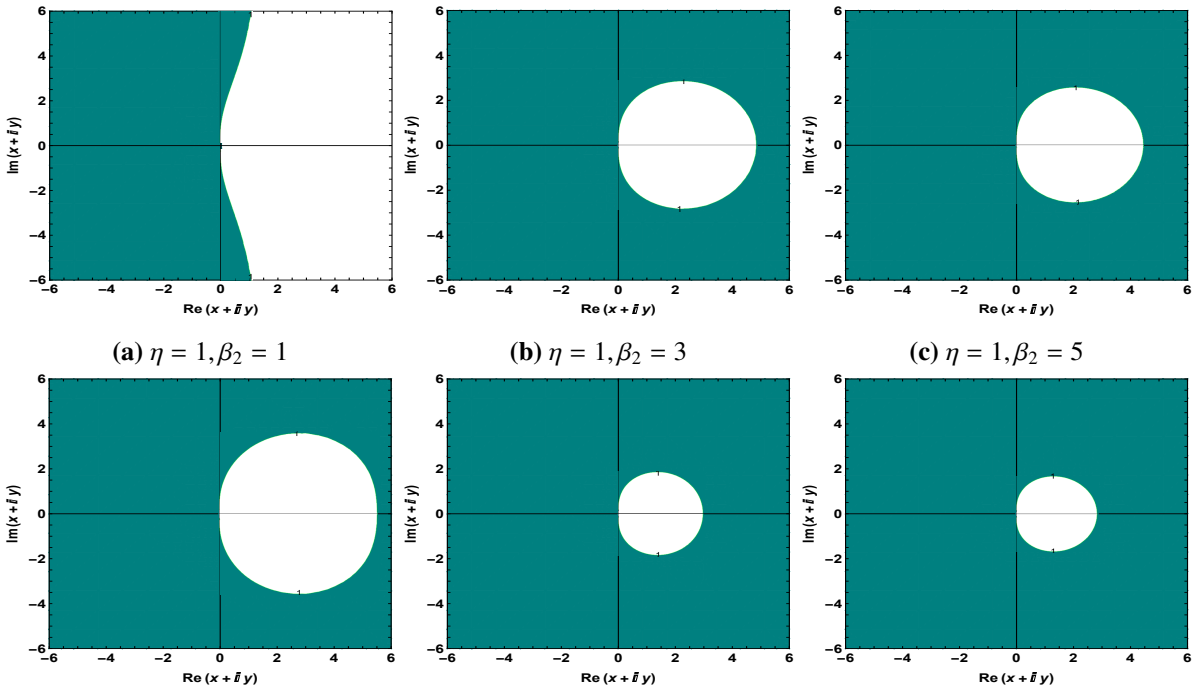

(a) $\eta = 1, \beta_2 = 1$ **(b)** $\eta = 1, \beta_2 = 3$ **(c)** $\eta = 1, \beta_2 = 5$

(d) $\eta = 2, \beta_2 = 1$ **(e)** $\eta = 2, \beta_2 = 3$ **(f)** $\eta = 2, \beta_2 = 5$

Figure 3. A-stability regions with different stability parameters η and β_2. (a) and (d): The classical BDF-DC$_2^3$ scheme; (b), (c), (e), and (f): The novel BDF-DC$_2^3$ scheme.

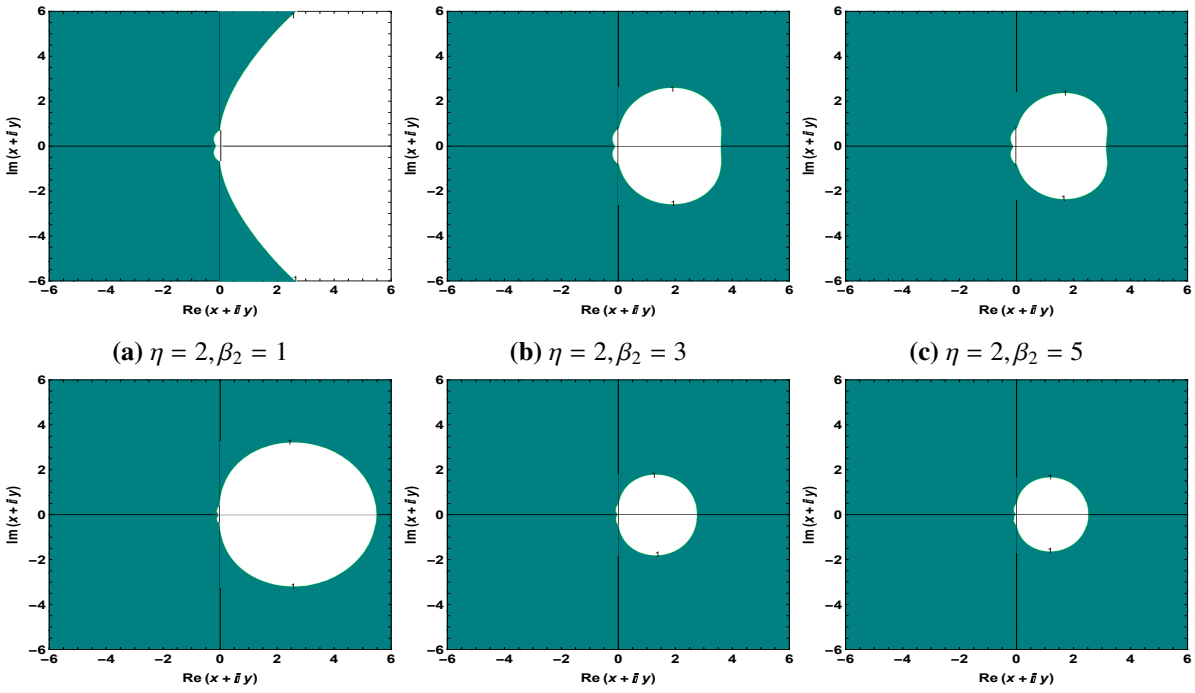

(a) $\eta = 2, \beta_2 = 1$ **(b)** $\eta = 2, \beta_2 = 3$ **(c)** $\eta = 2, \beta_2 = 5$

(d) $\eta = 4, \beta_2 = 1$ **(e)** $\eta = 4, \beta_2 = 3$ **(f)** $\eta = 4, \beta_2 = 5$

Figure 4. Stiff-stability regions with different stability parameters η and β_2. (a) and (d): The classical BDF-DC$_3^4$ scheme; (b), (c), (e), and (f): The novel BDF-DC$_3^4$ scheme.

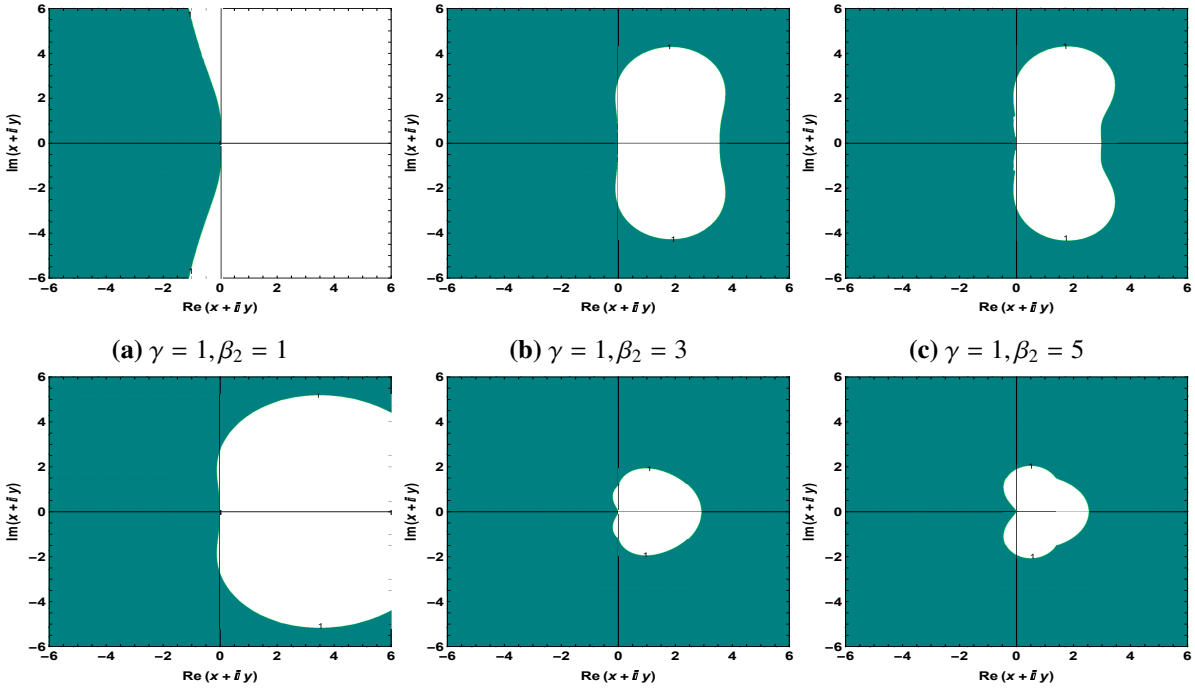

(a) $\gamma = 1, \beta_2 = 1$ **(b)** $\gamma = 1, \beta_2 = 3$ **(c)** $\gamma = 1, \beta_2 = 5$

(d) $\gamma = 3, \beta_2 = 1$ **(e)** $\gamma = 3, \beta_2 = 3$ **(f)** $\gamma = 3, \beta_2 = 5$

Figure 5. A(α)-stability regions with different stability parameters γ and β_2. (a) and (d): The classical BDF-DC$_2^4$ scheme; (b), (c), (e), and (f): The novel BDF-DC$_2^4$ scheme.

4. Numerical experiments

This section presents the numerical accuracy and examines the stability of the novel BDF-DC schemes for solving stiff systems.

Example 1. We take into account the following stiff system without source terms:

$$\begin{cases} \phi_1' = 998\phi_1 + 1998\phi_2, \quad \phi_1(0) = 1, \quad t \in [0, T], \\ \phi_2' = -999\phi_1 - 1999\phi_2, \quad \phi_2(0) = 0, \end{cases} \tag{4.1}$$

with the exact solution as follows:

$$\begin{cases} \phi_1(t) = 2e^{-t} - e^{-1000t}, \\ \phi_2(t) = -e^{-t} + e^{-1000t}. \end{cases} \tag{4.2}$$

In Table 2, we present the L^∞ errors and convergence orders of the novel BDF-DC schemes at point $t = 10$ for Eq (4.1) in ϕ_1. In Table 3, we report the L^∞ errors and convergence rates of the novel BDF-DC schemes at $T = 1$. The L^∞ errors are defined as the maximum absolute error over all time points t. Figures 6 and 7 illustrate the L^∞ error and convergence comparison for different schemes, where the parameters are chosen to be the same as those in Tables 2 and 3, respectively. It is evident that most of the schemes achieve their optimal orders. Notably, the BDF-DC$_3^4$ scheme is an exception, as it exhibits theoretical instability for relatively small time steps. We can observe from Tables 2 and 3 that although larger time-step sizes may lead to increase numerical errors, our proposed novel schemes still maintain high-order accuracy even for relatively larger time steps. Therefore, we adopt larger time-step sizes in the BDF-DC schemes, since the resulting increase in numerical errors is insignificant. These numerical results indicate that the fourth-order BDF-DC schemes achieve smaller numerical errors with larger time step sizes than the third-order BDF-DC schemes when the stability parameters specified in Table 1 are used for all schemes.

To validate the stability thresholds outlined in Table 1, we evaluate the proposed schemes with $\Delta t = \frac{1}{20}$ and perform simulations up to $T = 80$. Table 4 presents the corresponding stability thresholds for ϕ_1. Figure 8 depicts the analytical and numerical solutions comparison for different novel BDF-DC schemes. We can observe from Figure 8 that the numerical solutions for most schemes can better approximate the exact solution, and can also approximate well at the tip. However, for the BDF-DC$_2^4$ scheme, its solution at the tip cannot approximate well, the primary reason may be A(α)-stability influence. We can conclude from Table 4 that the proposed BDF-DC schemes become unstable when the values drop below the thresholds specified in Table 1. We can also observe that the stability of the novel BDF-DC schemes can be enhanced by increasing β_1 and β_2 values compared with the classical BDF-DC schemes. For the numerical solution ϕ_2, we can obtain similar results.

Example 2. We consider the following stiff problems with source terms:

$$\begin{cases} \phi_1' = 32\phi_1 + 66\phi_2 + \frac{2}{3}t + \frac{2}{3}, \quad \phi_1(0) = \frac{1}{3}, \quad t \in [0, T], \\ \phi_2' = -66\phi_1 - 133\phi_2 - \frac{1}{3}t - \frac{1}{3}, \quad \phi_2(0) = \frac{1}{3}, \end{cases} \tag{4.3}$$

and the exact solution is provided by

$$\begin{cases} \phi_1(t) = \dfrac{2}{3}t + \dfrac{2}{3}e^{-t} - \dfrac{1}{3}e^{-100t}, \\ \phi_2(t) = -\dfrac{1}{3}t - \dfrac{1}{3}e^{-t} + \dfrac{2}{3}e^{-100t}. \end{cases} \tag{4.4}$$

Figures 9 and 10 depict the L^∞ errors and convergence rates of the proposed BDF-DC schemes for Example 2. The schemes achieve the expected numerical accuracy. It is also demonstrated that stiff systems with source terms can be well approximated by the proposed schemes. Figure 11 shows a comparison between the exact and numerical solutions obtained by the proposed schemes for Eq (4.3). It can be observed that the numerical solution agrees very well with the exact solution. Figure 12 illustrates the evolution of the L^∞ errors over time t. We observe that the errors near the tip remain small, indicating that the proposed schemes are capable of accurately simulating problems with source terms. In addition, for nonlinear stiff systems, in order to avoid loss of accuracy, the implicit BDF-DC scheme may need to be reformulated as a semi-implicit scheme, or an appropriate iterative solver should be incorporated. This will be investigated in future work.

Table 2. L^∞ errors and the convergence rates of the novel BDF-DC schemes with $\beta_1 = \beta_2 = 3, T = 10$ in Example 1 for ϕ_1.

	BDF-DC$_3^3$		BDF-DC$_5^4$		BDF-DC$_2^3$		BDF-DC$_3^4$		BDF-DC$_2^4$	
Δt	$\alpha_1 = \frac{1}{2}$		$\alpha_1 = \frac{1}{2}, \alpha_2 = \frac{1}{2}$		$\eta = \frac{3}{2}$		$\eta = 3$		$\gamma = 2$	
	Error		Error		Error		Error		Error	
1/1280	1.89×10^{-14}	-	3.83×10^{-18}	-	9.61×10^{-14}	-	1.05×10^{-14}	-	8.50×10^{-17}	-
1/2560	2.36×10^{-15}	2.99	2.39×10^{-19}	4.00	1.20×10^{-14}	2.99	3.58×10^{-16}	4.83	5.32×10^{-18}	3.99
1/5120	2.95×10^{-16}	2.99	1.49×10^{-20}	4.00	1.50×10^{-15}	2.99	1.24×10^{-17}	4.87	3.32×10^{-19}	3.99
1/10240	3.69×10^{-17}	2.99	9.34×10^{-22}	4.00	1.88×10^{-16}	2.99	4.47×10^{-19}	4.79	2.08×10^{-20}	3.99
1/20480	4.61×10^{-18}	2.99	5.84×10^{-23}	4.00	2.35×10^{-17}	2.99	1.75×10^{-20}	4.67	1.30×10^{-21}	3.99
1/40960	5.77×10^{-19}	3.00	3.65×10^{-24}	4.00	2.94×10^{-18}	3.00	Inf	-	8.11×10^{-23}	4.00

Table 3. L^∞ errors and the convergence rates of the novel BDF-DC schemes with $\beta_1 = \beta_2 = 3, T = 1$ in Example 1 for ϕ_1.

	BDF-DC$_3^3$		BDF-DC$_5^4$		BDF-DC$_2^3$		BDF-DC$_3^4$		BDF-DC$_2^4$	
Δt	$\alpha_1 = \frac{1}{2}$		$\alpha_1 = \frac{1}{2}, \alpha_2 = \frac{1}{2}$		$\eta = \frac{3}{2}$		$\eta = 3$		$\gamma = 2$	
	Error		Error		Error		Error		Error	
1/1280	1.23×10^{-3}	-	9.02×10^{-4}	-	1.96×10^{-2}	-	1.81×10^{-2}	-	1.08×10^{-2}	-
1/2560	3.80×10^{-4}	1.69	7.52×10^{-5}	3.59	3.15×10^{-3}	2.63	2.53×10^{-3}	2.84	1.21×10^{-3}	3.16
1/5120	7.55×10^{-5}	2.33	5.47×10^{-6}	3.78	4.74×10^{-4}	2.73	2.90×10^{-4}	3.13	9.20×10^{-5}	3.72
1/10240	1.18×10^{-5}	2.67	3.62×10^{-7}	3.92	6.69×10^{-5}	2.83	2.75×10^{-5}	3.40	6.90×10^{-6}	3.74
1/20480	1.66×10^{-6}	2.83	2.32×10^{-8}	3.97	8.90×10^{-6}	2.91	2.19×10^{-6}	3.65	4.76×10^{-7}	3.86
1/40960	2.20×10^{-7}	2.92	1.46×10^{-9}	3.98	1.15×10^{-6}	2.95	Inf	-	3.13×10^{-8}	3.93

Table 4. Stability thresholds for the proposed novel methods with $\beta_1 = 1, \beta_2 = 3, \Delta t = \frac{1}{20}$ in Example 1 for ϕ_1.

BDF-DC$_3^3$	$\alpha_1 = 0.34$ Error 6.41×10^{40}	$\alpha_1 = 0.37$ Error 7.19×10^{-39}	$\alpha_1 = 0.40$ Error 1.12×10^{-38}	$\alpha_1 = 0.50$ Error 2.46×10^{-38}
BDF-DC$_5^4$	$\alpha_1 = 0.34, \alpha_2 = 0.20$ Error 1.29×10^{11}	$\alpha_1 = 0.37, \alpha_2 = 0.32$ Error 1.24×10^{-40}	$\alpha_1 = 0.40, \alpha_2 = 0.33$ Error 7.70×10^{-41}	$\alpha_1 = 0.50, \alpha_2 = 0.34$ Error 1.85×10^{-40}
BDF-DC$_2^3$	$\eta = 0.72$ Error 5.01×10^{10}	$\eta = 0.74$ Error 3.66×10^{-19}	$\eta = 1$ Error 5.16×10^{-34}	$\eta = 2$ Error 1.08×10^{-37}
BDF-DC$_3^4$	$\eta = 1.60$ Error 2.40×10^{0}	$\eta = 3.00$ Error 8.43×10^{-12}	$\eta = 4.00$ Error 1.10×10^{-23}	$\eta = 6.00$ Error 6.58×10^{-38}
BDF-DC$_2^4$	$\gamma = 0.56$ Error 1.80×10^{26}	$\gamma = 0.58$ Error 2.27×10^{-22}	$\gamma = 1.00$ Error 1.71×10^{-39}	$\gamma = 2.00$ Error 4.41×10^{-39}

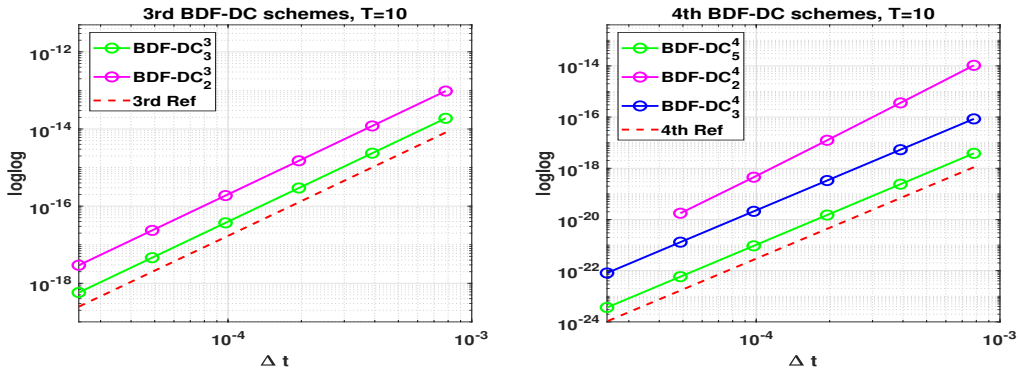

Figure 6. (Example 1) Comparison of L^∞ errors and convergence rates for different novel BDF-DC schemes with $T = 10$ for ϕ_1.

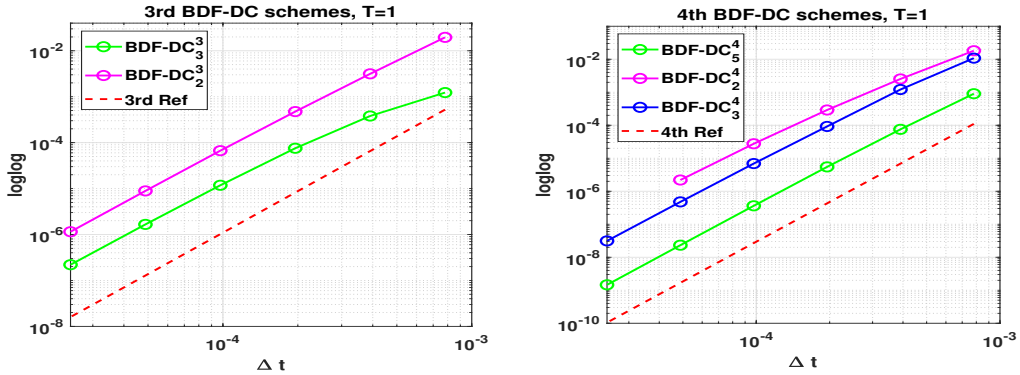

Figure 7. (Example 1) Comparison of L^∞ errors and convergence rates for different novel BDF-DC schemes with $T = 1$ for ϕ_1.

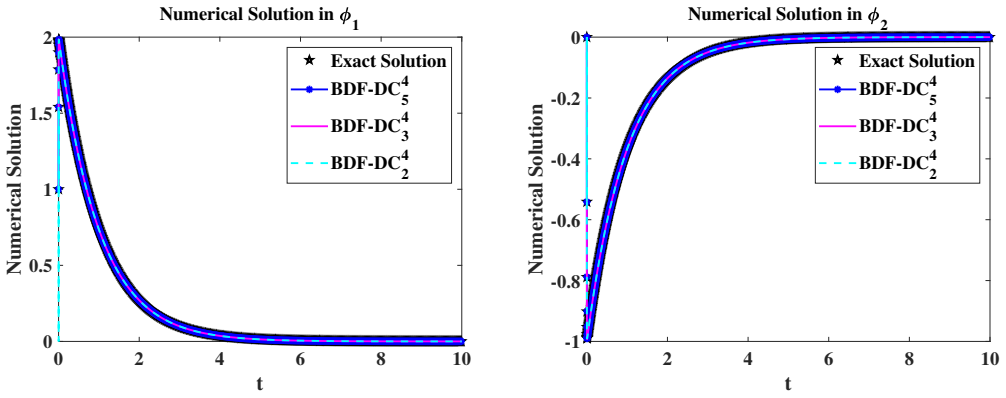

Figure 8. (Example 1) The analytical and numerical solutions comparison for different BDF-DC schemes with $T = 10$ and $\Delta t = \frac{1}{1280}$. Left: the novel BDF-DC schemes for ϕ_1; Right: the novel BDF-DC schemes for ϕ_2.

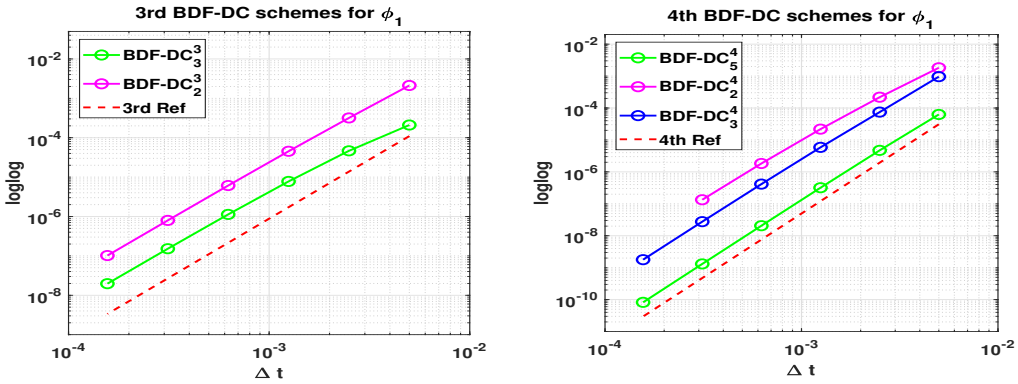

Figure 9. (Example 2) Comparison of L^∞ errors and convergence rates for different novel BDF-DC schemes with $T = 1$ for ϕ_1.

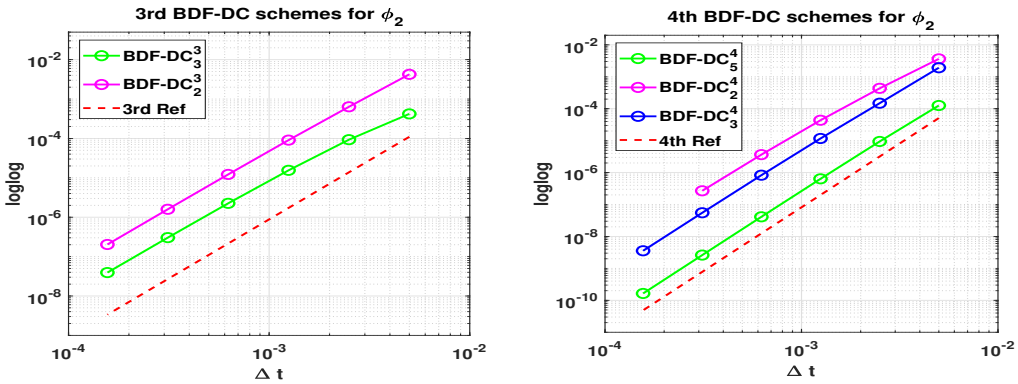

Figure 10. (Example 2) Comparison of L^∞ errors and convergence rates for different proposed BDF-DC schemes with $T = 1$ for ϕ_2.

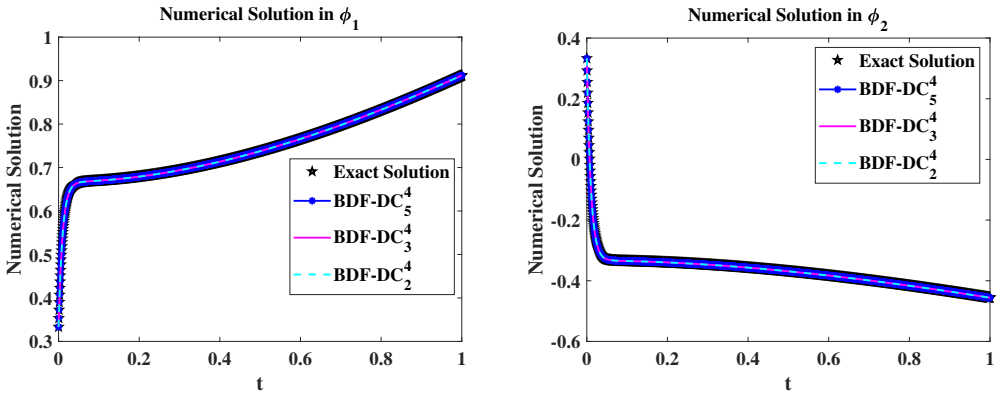

Figure 11. (Example 2) The analytical and numerical solutions comparison for different BDF-DC schemes with $T = 1$ and $\Delta t = \frac{1}{1600}$. Left: the novel BDF-DC schemes for ϕ_1; Right: the novel BDF-DC schemes for ϕ_2.

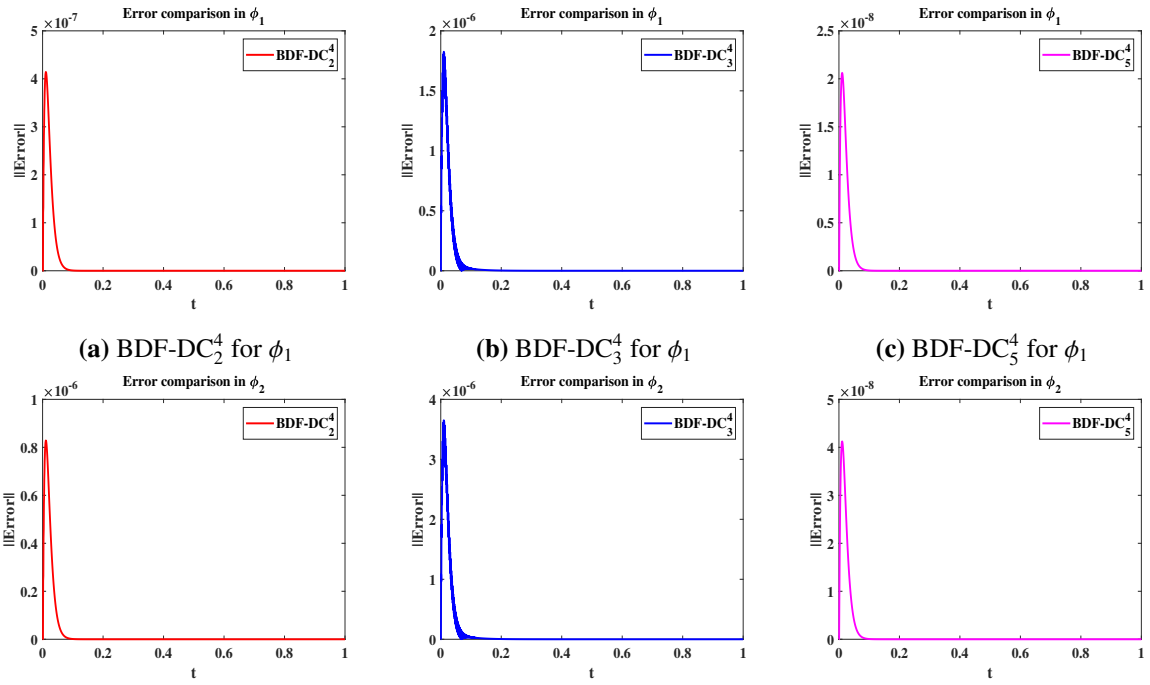

(a) BDF-DC$_2^4$ for ϕ_1 **(b)** BDF-DC$_3^4$ for ϕ_1 **(c)** BDF-DC$_5^4$ for ϕ_1

(d) BDF-DC$_2^4$ for ϕ_2 **(e)** BDF-DC$_3^4$ for ϕ_2 **(f)** BDF-DC$_5^4$ for ϕ_2

Figure 12. (Example 2) The temporal evolution of the L^∞ errors for the proposed BDF-DC schemes with $T = 1$ and $\Delta t = \frac{1}{1600}$. (a)-(c) The BDF-DC schemes in ϕ_1; (d)-(e) The BDF-DC schemes in ϕ_2.

5. Conclusions

In this paper, we presented several novel A-stable, high-order schemes, which integrate the DC framework with advanced BDF methods. The primary benefit of the these new BDF schemes was that they not only improved the stability of classical BDF methods, but also elevated the stable areas of the proposed novel methods. Additionally, we meticulously explored how to choose the

stability values in the schemes, with the goal of further optimizing the stability characteristics of the proposed schemes.

Use of AI tools declaration

The authors declare they have not used Artificial Intelligence (AI) tools in the creation of this article.

Acknowledgements

The authors are very grateful to the referee for carefully reading the article and providing many valuable comments.

Conflict of interest

The authors declare no conflicts of interest.

Author contributions

Conceptualization, L. Y.; software, L. Y. and X. L.; formal analysis, L. Y. and X. Z.; writing-original draft preparation, L. Y.; writing-review and editing, L. Y. and X. Z.; visualization, L. Y. and X. Z. All authors have read and agreed to the published version of the manuscript.

Availability of data and material

The data analyzed in this study are subject to the following licenses/restrictions: The first author can receive the restrictions. Requests to access these data sets should be directed to yaolin1023@ustc.edu (L. Yao).

Funding

The research of was partially supported by the Doctoral Research Foundation of Xinjiang Normal University (No. XJNUZBS2509), and the Natural Science Foundation of Xinjiang (No. 2025D01B74).

References

1. J. D. Lambert, Numerical methods for ordinary differential systems, *Wiley New York*, 1991.
2. S. Boscarino, J. M. Qiu, G. Russo, Implicit-explicit integral deferred correction methods for stiff problems, *SIAM J. Sci. Comput*, **40** (2018), A787–A816. https://doi.org/10.1137/16M1105232
3. S. A. M. Yatim, Z. B. Ibrahim, K. I. Othman, M. B. Suleiman, A quantitative comparison of numerical method for solving stiff ordinary differential equations, *Math. Probl. Eng*, **2011** (2011), 193691. https://doi.org/10.1155/2011/193691
4. G. Wanner, E. Hairer, *Solving Ordinary Differential Equations II*, Springer Berlin Heidelberg New York, 1996.

5. R. K. Alexander, J. J. Coyle, Runge-Kutta methods and differential-algebraic systems, *SIAM J. Numer. Anal.*, **27** (1990), 736–752. https://doi.org/10.1137/0727043
6. A. Kværnø, S. P. Nørsett, B. Owren, Runge-Kutta research in trondheim, *Appl. Numer. Math.*, **22** (1996), 263–277. https://doi.org/10.1016/S0168-9274(96)00037-2
7. R. I. Okuonghae, M. N. O. Ikhile, A(α)-Stable linear multistep methods for stiff IVPs in ODEs, *Acta Univ. Palacki. Olomuc., Fac. Rer. Nat., Math.*, **50** (2011), 73–90. Available from: http://dml.cz/dmlcz/141714.
8. A. Bouchriti, M. Pierre, N. E. Alaa, Gradient stability of high-order BDF methods and some applications, *J. Differ. Equ. Appl.*, **26** (2020), 74–103. https://doi.org/10.1080/10236198.2019.1709062
9. A. Sreedhar, M. K. Yadav, C. Satyanarayana, RBF based backward differentiation methods for stiff differential equations, *Eng. Anal. Bound. Elem.*, **176** (2025), 106215. https://doi.org/10.1016/j.enganabound.2025.106215
10. G. G. Dahlquist, A special stability problem for linear multistep methods, *BIT Numer. Math.*, **3** (1963), 27–43. https://doi.org/10.1007/BF01963532
11. L. Yao, Y. H. Xia, Y. Xu, Stability of implicit deferred correction methods based on BDF methods, *Appl. Math. Lett.*, **158** (2024), 109255. https://doi.org/10.1016/j.aml.2024.109255
12. K. Böhmer, H. J. Stetter, Defect correction methods, *Theory Appl.*, **5** (1984).
13. A. Dutt, L. Greengard, V. Rokhlin, Spectral deferred correction methods for ordinary differential equations, *BIT Numer. Math.*, **40** (2000), 241–266. https://doi.org/10.1023/A:1022338906936
14. M. L. Minion, Semi-implicit spectral deferred correction methods for ordinary differential equations, *Commun. Math. Sci*, **1** (2003), 471–500. https://doi.org/10.4310/CMS.2003.v1.n3.a6
15. A. T. Layton, On the choice of correctors for semi-implicit Picard deferred correction methods, *Appl. Numer. Math.*, **58** (2008), 845–858. https://doi.org/10.1016/j.apnum.2007.03.003
16. R. Guo, Y. Xu, Semi-implicit spectral deferred correction methods based on second order time integration schemes for nonlinear PDEs, *J. Comput. Math.*, **42** (2024), 111–133. https://doi.org/10.4208/jcm.2202-m2021-0302
17. L. Yao, Y. H. Xia, Y. Xu, L-stable spectral deferred correction methods and applications to phase field models, *Appl. Numer. Math.*, **197** (2024), 288–306. https://doi.org/10.1016/j.apnum.2023.11.020
18. S. C. E. R. Koyaguerebo-Imé, Sixth-order explicit one-step methods for stiff ODEs via hybrid deferred correction involving RK2 and RK4: Application to reaction-diffusion equations, preprint, arXiv: 2512.18377, 2025. https://doi.org/10.48550/arXiv.2512.18377
19. F. K. Huang, J. Shen, On a new class of BDF and IMEX schemes for parabolic type equations, *SIAM J. Numer. Anal.*, **62** (2024), 1609–1637. https://doi.org/10.1137/23M1612986

20. J. J. H. Miller, On the location of zeros of certain classes of polynomials with applications to numerical analysis, *IMA J. Appl. Math.*, **8** (1971), 397–406. https://doi.org/10.1093/imamat/8.3.397